Cerebral Cortex August 2013;23:1874–1883
doi:10.1093/cercor/bhs175
Advance Access publication July 4, 2012

Dissecting the Anticipation of Aversion Reveals Dissociable Neural Networks

Daniel W. Grupe[1,2], Desmond J. Oathes[1,4] and Jack B. Nitschke[1,2,3]

[1]Waisman Laboratory for Brain Imaging and Behavior, [2]Department of Psychology, [3]Department Psychiatry, University of Wisconsin-Madison, Madison, WI 53705-2280, USA and [4]Department of Psychiatry and Behavioral Sciences, Stanford University, Stanford, CA, USA

Address correspondence to: Daniel W. Grupe, Waisman Laboratory for Brain Imaging and Behavior, University of Wisconsin-Madison, 1500 Highland Avenue, Madison, WI 53705-2280, USA. Email: grupe@wisc.edu

The anticipation of future adversity confers adaptive benefits by engaging a suite of preparatory mechanisms, but this process can also be deleterious when carried out in excess. Neuroscientific investigations have largely treated anticipation as a unitary process, but we show here using functional magnetic resonance imaging that distinct stages of aversive anticipation are supported by dissociable neural mechanisms. Immediate anticipatory responses were observed in regions associated with threat detection and early processing of predictive cues, including the orbitofrontal cortex and pregenual anterior cingulate cortex, as well as the amygdala for individuals with elevated anxiety symptoms. Sustained anticipatory activity was observed in the forebrain/bed nucleus of the stria terminalis, anterior insula, anterior mid-cingulate cortex (aMCC), and midbrain/periaqueductal gray, regions associated with anxiety, interoception, and defensive behavior. The aMCC showed increased functional coupling with the midbrain during sustained anticipation of aversion, highlighting a circuit critical for the expression of preparatory fear responses. These data implicate distinct sets of regions that are active during different temporal stages of anticipation, and provide insight into how the human brain faces the future both adaptively and maladaptively.

Keywords: amygdala, anterior insula, BNST, fMRI, rostral cingulate

Introduction

As human beings we spend much of our waking hours living out the future in advance of its actual occurrence, a distinctly human trait that can confer myriad benefits to those who do it well. In particular, the anticipation of future adversity serves an adaptive purpose by engaging preparatory behavioral, cognitive, and affective mechanisms. While such anticipatory processing ideally allows individuals to minimize physical and psychological harms, it can paradoxically be deleterious when its engagement is excessive relative to the actual threat faced by the individual. Taken to an extreme, such exaggerated anticipatory processing can contribute to the development or maintenance of clinical anxiety disorders (Barlow 2000; Borkovec 2002; Nitschke et al. 2009).

Given the important adaptive benefits of effective anticipatory processing, and the negative consequences resulting from excessive anticipation of harm, a multitude of functional magnetic resonance imaging (fMRI) studies have investigated the neural circuitry recruited during the anticipation of aversive events (e.g., negative emotional images, painful stimulation, electric shock). Over a decade of research has outlined a number of regions consistently engaged by these tasks, including the anterior insula, pregenual anterior cingulate cortex (pACC) and anterior mid-cingulate cortex (aMCC), dorsomedial and dorsolateral prefrontal cortex (PFC), orbitofrontal cortex (OFC), amygdala, extended amygdala areas such as the bed nucleus of the stria terminalis (BNST), and midbrain regions such as the periaqueductal gray (PAG; Ploghaus et al. 1999; Wager et al. 2004; Nitschke et al. 2006; Herwig et al. 2007; Mechias et al. 2010; Drabant et al. 2011).

Despite the volume of research conducted on this topic, few studies have taken steps to decompose the broad construct of "anticipation" into its multiple constituent processes, including threat detection, increased attention and arousal, induction and regulation of negative affective states, cognitive restructuring, and initiation of preparatory avoidant motor responses (Nitschke et al. 2006). Importantly, such processes are unlikely to occur simultaneously, but may unfold serially or on different time scales. In treating anticipation as a unitary process both descriptively and statistically, the extant literature is lacking a comprehensive description of how these distinct stages of anticipation are represented in the brain. The conceptualization and modeling of anticipation as a singular, unitary process may result in inconsistent replication efforts and slow the advance of research on the topic.

In the current study, we focused specifically on the neural instantiation of different temporal stages of anticipation in a group of 43 subjects, utilizing an approach designed to identify patterns of activation with qualitatively distinct characteristics. Namely, we conceptualized and modeled the anticipation of negative events as consisting of 1) immediate phasic responses to cues signaling an upcoming aversive or neutral picture and 2) sustained anticipatory responses leading up to the presentation of that picture. This framework is conceptually similar to electroencephalography studies that have examined separate orienting responses to warning cues and subsequent stimulus-preceding negativity in anticipation of emotionally valenced stimuli (Birbaumer et al. 1990; Böcker et al. 2001). Previous fMRI studies that have modeled distinct phases of anticipation either have divided the anticipatory epoch into early and late periods using boxcar regressors of roughly equal length (Phelps et al. 2001; Wager et al. 2004; Kumari et al. 2007), or have used a similar approach to that implemented here but reported effects corresponding only to 1 of these 2 anticipatory regressors (Kalisch et al. 2005, 2006; Carlson et al. 2011). In contrast, we sought to thoroughly delineate the brain areas associated with each of these 2 stages of anticipation by conducting whole-brain analyses for the phasic and sustained regressors, as well as region-of-interest (ROI) analyses in several a priori regions (noted below). These primary analyses were supplemented with the investigation of individual differences and task-modulated functional connectivity. Our explicit motivation to parse anticipatory neural activity into distinct temporal stages, combined with our large sample size and multiple,

complementary analytic techniques, allowed for a comprehensive characterization of the neural basis of distinct phasic and sustained anticipatory processes.

Based on nonhuman animal literature and human neuroimaging research, we hypothesized a dissociation for amygdala and BNST activation. Greater phasic anticipatory responses were expected for the amygdala due to its role in vigilance and threat detection (LeDoux 2000; Davis and Whalen 2001), whereas greater sustained anticipatory activity was predicted for the closely related and heavily interconnected BNST, which is recruited during conditions of generalized anxiety and sustained threat (Davis et al. 2010; Somerville et al. 2010, 2012; Alvarez et al. 2011). We also investigated the temporal response profile of the pACC and aMCC sectors of the rostral cingulate cortex, a structurally and functionally heterogeneous region that is frequently active during anticipation of aversion (Mechias et al. 2010). In particular, we predicted that the aMCC would demonstrate sustained anticipatory activity, due to its engagement by conditions of sustained or looming threat (Kalisch et al. 2006; Straube et al. 2009; Mobbs et al. 2010). Functional connectivity analyses were implemented using the aMCC as a seed region based on this region's hypothesized role in directing or regulating preparatory defensive behavior (Shackman et al. 2011). Finally, anterior insula activity was expected to be greater for sustained anticipation, based on this region's role in subjective emotional awareness and interoception (Craig 2002, 2009; Critchley et al. 2004; Somerville et al. 2012).

Materials and Methods

Participants

Participants for this study were 45 healthy subjects recruited from flyers on the University of Wisconsin-Madison campus and the surrounding Madison community. Following the loss of data from 2 subjects due to corrupted stimulus timing files, our final sample consisted of 43 subjects (mean age = 24.2 ± 6.7 years, 22 females, all right-handed). Participants were free of any current or past history of psychiatric disease as determined by administration of a Structured Clinical Interview for DSM-IV (First et al. 2002) and were not currently using medication to treat any psychiatric disorders. All study procedures were carried out in accordance with policies and procedures of the University of Wisconsin-Madison Health Sciences Institutional Review Board, and participants were monetarily compensated at the completion of the study.

Experimental Paradigm

fMRI data were collected during an emotional anticipation task using aversive and neutral pictures from the International Affective Picture System (IAPS; Lang et al. 2008) (Fig. 1). One of 3 visual cues informed participants that the following picture would be aversive ("X"), neutral ("O"), or either aversive or neutral ("?"). Each cue was presented for 2 s, followed by a 2- to 8-s jittered inter-stimulus interval (ISI), a 1-s picture presentation, an additional 5- to 9-s ISI, and a 6-s period during which participants rated either their current mood or the valence of the previous picture on a Likert scale from −4 (unpleasant/negative) to +4 (pleasant/happy). These 2 types of ratings were counterbalanced across conditions. A 1- to 5-s jittered inter-trial interval preceded the onset of the next trial. Each of 4 experimental runs (~12:00 each) consisted of 8 aversive trials, 8 neutral trials, and 8 uncertain trials, which were presented in a pseudorandom order, for a total of 32 trials of each condition type over the course of the experiment. In addition to these standard trials, there were 2 additional trial types that occurred less frequently. First, there were a total of 6 presentations of each of the 3 cues that were not followed by a picture stimulus; instead, immediately following the 5- to 9-s ISI, participants rated their current anxiety on a Likert scale from 0 (not at all anxious) to 8 (extremely anxious). Secondly, there were a total of 6 aversive and 6 neutral pictures that were not preceded by a cue stimulus; instead, these trials began with a picture presentation followed by the 5- to 9-s ISI and the mood or valence rating scales described above.

Data Acquisition

Magnetic resonance images were acquired on a 3.0 Tesla GE SIGNA scanner with a quadrature birdcage head coil. Whole-brain functional scans were collected using T_2*-weighted echo-planar images (EPI; 30 interleaved sagittal slices, repetition time [TR] = 2000 ms, echo time [TE] = 30 ms, flip angle [α] = 30°, field of view [FOV] = 240 mm^2, matrix = 64 × 64, in-plane resolution = 3.75 mm^2, slice thickness = 4.0 mm, slice gap = 1.0 mm). To correct for the field-map distortion, 4 additional EPI runs were acquired with identical acquisition parameters but with TEs of 30, 31, 33, and 36 ms. Whole-brain anatomical images were collected for coregistration of functional data across subjects using an axial T_1-weighted spoiled gradient-recalled echo scan (TR = 35 ms, TE = 8 ms, α = 30°, FOV = 240 mm^2, matrix = 256 × 192, slice thickness = 1.2 mm, 124 slices).

fMRI Processing, Analysis, and Statistics

The following data processing steps were implemented using AFNI version 2 (Cox 1996): Realignment to the initial volume, 6-parameter rigid body motion correction, slice timing correction, field-map correction, percent signal change normalization, and alignment of the T_1 anatomical image to the EPI data. The processed EPI data were analyzed using 2 separate general linear models (GLMs), which differed only with respect to the regressors used to model the blood oxygen level-dependent (BOLD) signal during the anticipatory epoch (Fig. 1*C*). For the "1-regressor" model, anticipatory activity for each condition was modeled using a single stick regressor at the onset of the cue. For the "2-regressor" model, phasic activity was modeled using the same stick regressor at the cue onset, and sustained anticipatory activity was modeled using a duration-modulated boxcar regressor spanning the entirety of the 2- to 8-s anticipatory ISI. Both models additionally included regressors corresponding to each type of the picture and rating period, as well as 6 motion covariates. Following construction of the design matrix for each subject, the BOLD signal for each event was modeled by convolving events with a canonical hemodynamic response function. We also tested an alternative version of the 2-regressor model, in which the boxcar regressor began at the cue onset (rather than the offset) and continued through the duration of the ISI. Results were nearly identical whether the sustained anticipatory period began at the cue onset or cue offset.

Each subject's T_1 image was transformed into Montreal Neurological Institute (MNI) atlas space using an iterative nonlinear transformation algorithm (FNIRT; http://www.fmrib.ox.ac.uk/fsl/fnirt/index.html). This nonlinear registration process resulted in improved between-subject coregistration relative to linear registration, which allowed for the use of a smaller spatial smoothing filter and improved power to identify activation in smaller subcortical structures. The resulting nonlinear warp was applied to the beta maps resulting from each subject's GLM, voxels were resampled to 2 × 2-mm resolution, and a 4-mm full-width half-maximum isotropic Gaussian smoothing kernel was applied to the co-registered functional data.

Group analysis of the fMRI data focused on the comparison of the aversive and neutral conditions during the anticipatory epoch. This contrast provided the most robust differences, in terms of psychological states and associated neural activity, for achieving the primary study goal of dissecting anticipatory activity into distinct phasic and sustained components. Anticipatory activity associated with the uncertain cue ("?") showed few differences from the neutral condition for either the phasic or sustained conditions, and there was only 1 region in which the uncertain condition showed greater activity than the aversive condition. For completeness, results comparing the uncertain condition with the certain aversive and neutral conditions are provided as Supplementary Materials (Supplementary Tables S1–S4). Results of ancillary analyses comparing picture responses for the

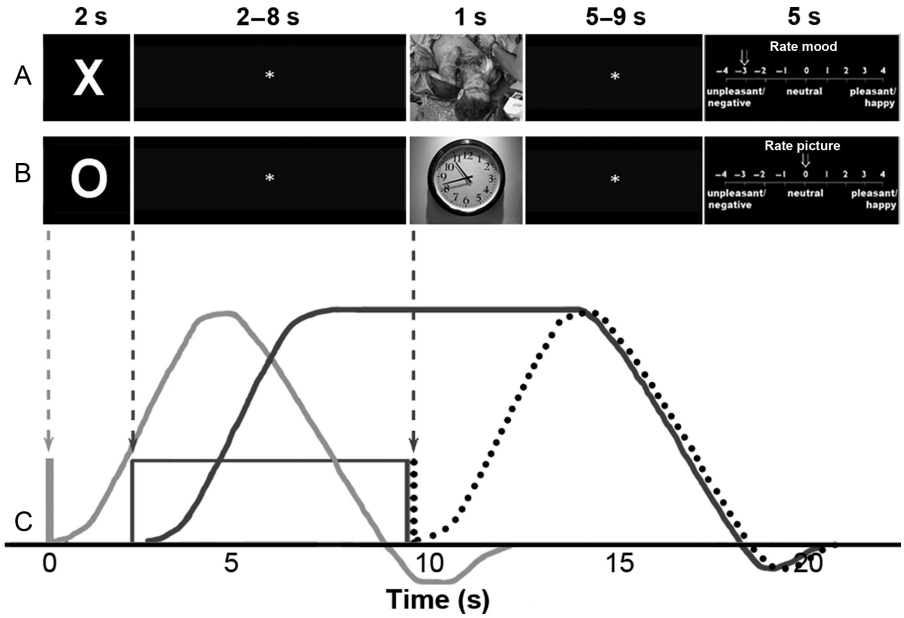

Figure 1. Schematic of the paradigm presented to subjects during fMRI scanning. (*A*) On aversive trials, subjects viewed an X cue for 2 s, followed by a 2- to 8-s ISI and an aversive picture for 1 s. Following a 5- to 9-s ISI, subjects rated either their mood or the picture valence. (*B*) Neutral trials had an identical structure to aversive trials, with an O cue preceding a neutral picture. (*C*) Modeling of the BOLD signal during anticipation included 2 distinct regressors, each of which was convolved with a standard hemodynamic response function: An event regressor at the onset of the anticipatory cue (light gray line and curve), and a boxcar regressor lasting the duration of the anticipatory ISI (dark gray box and curve). Responses during the picture period were modeled using an event regressor (dotted line and curve). The *x*-axis shows time (in seconds) from the trial onset.

1- and 2-regressor models are presented as Supplementary Materials (Supplementary Fig. S4).

For the 1-regressor model, the group analysis consisted of a single aversive versus neutral paired sample *t*-test. For the 2-regressor model, 2 separate paired sample *t*-tests were used: Aversive versus neutral phasic responses to the cue, and aversive versus neutral sustained anticipatory responses. The statistics resulting from multiple linear regression in AFNI are partial statistics, meaning that the significance of the aversive versus neutral cue contrast is calculated with variance attributed to sustained anticipatory activity removed, and vice versa. Thus, the results of the 2-regressor model reveal brain regions that are responsive for either the phasic or the sustained anticipation regressor, while taking into account activity associated with the other regressor.

Whole-brain, voxelwise statistics were calculated for each of the contrasts specified above for the 2 models of anticipatory activity. Correction for multiple comparisons was achieved by analyzing the results of each 2-tailed, paired sample *t*-test at an uncorrected threshold of $P < 0.005$ with a cluster threshold of 34 voxels (272 mm^3), which resulted in a corrected *P*-value of 0.05 (based on Monte Carlo simulation using AlphaSim in AFNI).

The rostral cingulate and amygdala were a priori ROIs due to their involvement in previous studies of aversive anticipation, yet whole-brain analyses failed to provide definitive evidence for their role in early or late stages of anticipation (see Results). To more completely probe the role of these regions in the context of the 2-regressor model, follow-up ROI analyses were conducted for these regions, using anatomical masks defined in MNI template space from the Harvard–Oxford probabilistic structural atlas (http://www.cma.mgh.harvard.edu/) with a 50% probability threshold. The posterior extent of the rostral cingulate mask was set at $y = 0$, based on anatomical and functional characteristics of the cingulate cortex (Shackman et al. 2011). The rostral cingulate mask was further divided into 2 distinct subregions: The pACC and the aMCC, using the genu of the corpus callosum ($y = 30$) as the dividing line along the *y*-axis (Vogt 2005). The mask did not include any of the subgenual cingulate, which is a separate mask region in the Harvard–Oxford atlas. The 50% probability amygdala ROIs were used without any further modifications. Parameter estimates for the aversive and neutral conditions were extracted from cingulate and amygdala ROIs for the phasic and sustained regressors separately, and submitted to repeated measures analyses of variance (ANOVAs): Valence (Aversive, Neutral) × Region (pACC, aMCC) × Period (Phasic, Sustained) for the cingulate and Valence (Aversive, Neutral) × Hemisphere (L, R) × Period (Phasic, Sustained) for the amygdala. Main effects and interactions were tested using a significance threshold of $P < 0.05$.

Individual differences in the magnitude of phasic and sustained activity for the aversive versus neutral contrast were correlated with 2 self-report measures: The Negative Affect subscale of the Positive and Negative Affect Schedule (PANAS; Watson et al. 1988) and the Penn State Worry Questionnaire (PSWQ; Meyer et al. 1990), each of which was administered immediately following the MRI scan. Pearson correlation coefficients were calculated between these self-report measures and mean parameter estimates extracted from clusters identified in the whole-brain analysis, as well as from each of the anatomical ROIs. To minimize the number of tests conducted, correlations were calculated only for a priori ROIs and activations in areas highlighted in previous work on the anticipation of aversion. To control the false positive rate for the number of tests corrected (10 brain regions correlated with both PANAS and PSWQ scores), we implemented false discovery rate (FDR) correction with a corrected threshold of $P < 0.05$. The 2-tailed *q*-values and associated *P*-values are both reported below. For each bivariate correlation, data points with studentized residuals corresponding to a Bonferroni-corrected $P < 0.05$ were considered outliers and were excluded from that correlation.

Based on aMCC activity during sustained aversive anticipation (see Results) and this region's proposed role in driving arousal states and fear expression (Critchley 2005, 2009; Milad et al. 2007; Shackman et al. 2011), context-dependent functional connectivity of the aMCC was assessed using psychophysiological interaction (PPI) (Friston et al. 1997). Time course data were extracted from a sphere with 8-mm radius centered on the aMCC voxel showing the greatest response during sustained anticipation of aversion (MNI coordinates: [3, 7, 33]), and terms associated with the baseline, linear drift, and head motion were removed. The 2-regressor GLM was applied again with 3 additional terms: The processed aMCC time series, the contrast of aversive versus neutral anticipation (during the 2- to 8-s anticipatory ISI), and the interaction of these 2 terms. Beta weights for the interaction term were converted to *Z*-scores to allow for across-subject comparison, and voxelwise 1-sample *t*-tests versus 0 were conducted

to identify voxels in which functional coupling with the aMCC differed during the anticipation of aversive versus neutral pictures. Correction for multiple comparisons was implemented in an identical fashion as for the voxelwise analyses described above. To test the specificity of the results to the aMCC, an analogous PPI analysis was implemented using the pACC as the seed region (MNI coordinates: [−2, 38, 14]). PPI analyses for phasic responses were not feasible due to the limited number of time points available to adequately assess functional connectivity.

Three sets of analyses were conducted to directly compare the 1- and 2-regressor models. First, we compared activity across the 2 models for the 2 sets of predictors common to both models: The phasic cue regressors and the picture regressors. This allowed us to demonstrate the extent to which explicitly modeling sustained anticipatory activity affected estimates of phasic anticipatory activity as well as picture-related activity. For each subject, aversive–neutral contrast estimates were calculated for the cue and picture regressors in each model. Voxelwise, paired sample *t*-tests were then conducted to reveal whole-brain differences in cue- or picture-related activity between the 2 models. Secondly, we conducted analyses to identify "new" variance accounted for by the 2-regressor model above and beyond that explained by the 1-regressor model. For each model, the overall model fit (R^2) was calculated at each voxel, and voxelwise, paired sample *t*-tests were conducted to test for an increase in overall variance accounted for in the 2-regressor model. Thirdly, we conducted within-region correlations between the anticipation regressor for the 1-regressor model and the phasic and sustained regressors from the 2-regressor model. Whole-brain multiple comparisons correction was carried out for each of these analyses using the same parameters as indicated above for our primary analyses.

Results

Self-Report Data

Self-reported anxiety was greater following the anticipatory epoch on trials cued with the aversive relative to the neutral cue ($t(42) = 4.11$, $P < 0.001$). For trials beginning with the uncertain cue, self-reported anxiety was greater than for neutral trials ($t(42) = 3.48$, $P = 0.0012$) and no different than for aversive trials ($t(42) = 0.98$, $P = 0.34$). Following the presentation of aversive relative to neutral pictures, participants rated their mood as more negative ($t(42) = 6.48$, $P < 0.001$), and also rated aversive pictures as more negative than neutral pictures ($t(42) = 6.47$, $P < 0.001$). These data demonstrate that the IAPS pictures were sufficiently aversive to induce negative mood and anticipatory anxiety.

One-Regressor Model: Whole-Brain Results

Whole-brain, voxelwise results for the contrast of aversive–neutral anticipation in the 1-regressor model were consistent with previous studies on the anticipation of aversion, and included activation of the bilateral anterior insula, rostral cingulate (spanning the pACC and aMCC), posterior subgenual cingulate, left OFC, left temporal pole, midbrain in the vicinity of the PAG, right precentral gyrus, posterior cingulate cortex (PCC), left superior parietal cortex, right fusiform gyrus, and early visual areas (Fig. 2, yellow/orange/green; Table 1). Greater activity for neutral relative to aversive anticipation was observed only in the cuneus.

Two-Regressor Model: Whole-Brain Results

Whole-brain, voxelwise activity for the contrast of aversive–neutral anticipation in the 2-regressor model revealed that early phasic anticipatory responses activated different brain areas than did the ensuing sustained anticipatory responses. Phasic responses to the cue were seen in the left OFC, left inferior frontal gyrus (IFG)/anterior insula, left temporal pole,

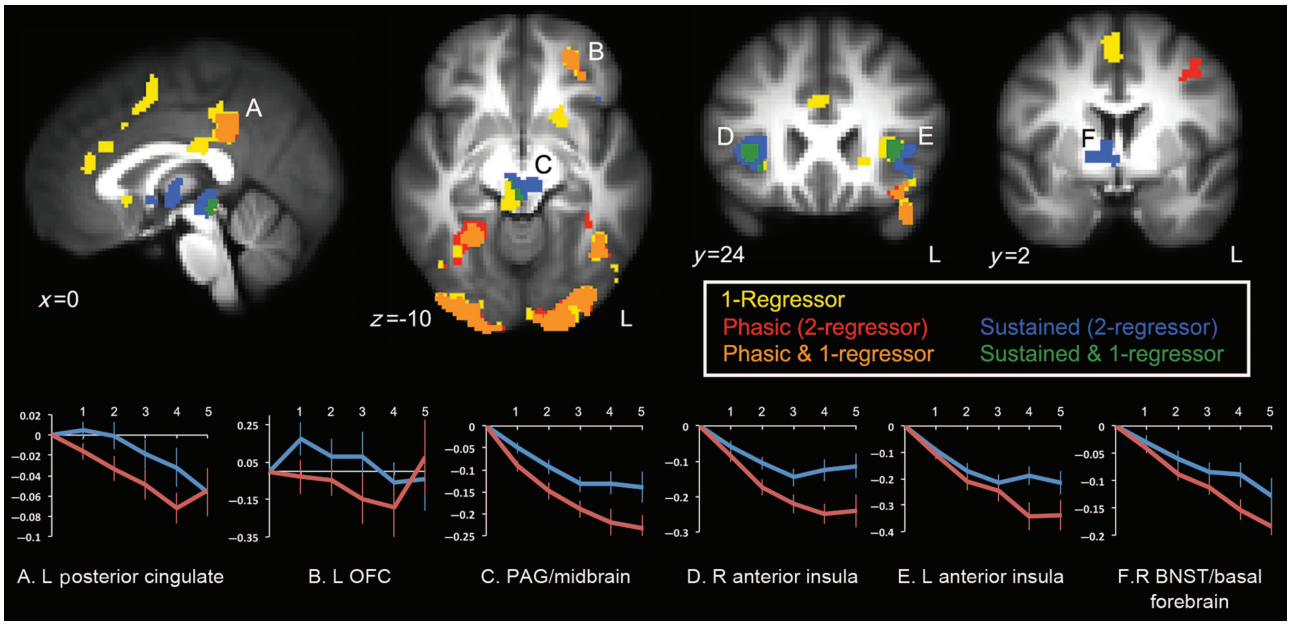

Figure 2. (Top panel) Anticipatory activation for the 1-regressor model (yellow), and phasic (red) and sustained anticipatory activation (blue) for the 2-regressor model at $P < 0.05$ (corrected using Monte Carlo simulation). Overlap between 1-regressor and phasic clusters is shown in orange; overlap between 1-regressor and sustained clusters is shown in green. Activation of the posterior cingulate (*A*) and the left OFC (*B*) in the 1-regressor model was attributed to the phasic regressor in the 2-regressor model. Activation of the midbrain/PAG (*C*) and bilateral anterior insula (*D*/*E*) in the 1-regressor model was attributed to the sustained regressor in the 2-regressor model. Sustained activity was observed in the right basal forebrain including the BNST (*F*), whereas no activity was observed in this region for the 1-regressor model. At the corrected threshold, neither regressor in the 2-regressor model independently accounted for the rostral cingulate activation in the 1-regressor model (Fig. 4*A* and Supplementary Fig. S1). (Bottom panel) Time course data extracted from clusters showing significant phasic (*A*,*B*) and sustained (*C*–*F*) activity. The *x*-axis reflects 2-s volumes from the cue onset and the *y*-axis reflects percent signal change from the baseline. The error bars (standard errors of the mean) increase in magnitude for later time points, which contained fewer averages.

left precentral gyrus, PCC, bilateral fusiform/parahippocampal cortex, and early visual areas (Fig. 2, red/orange; Table 2). Greater activity for the neutral cue was seen only in the cuneus.

In contrast, sustained anticipatory activity was greater for the aversive relative to the neutral condition in the bilateral anterior insula, right basal forebrain, midbrain, and right supramarginal gyrus (Fig. 2, blue/green; Fig. 3; Table 2). Greater activity for sustained neutral anticipation was seen only in the left angular gyrus. The basal forebrain cluster, which was not observed using the 1-regressor model, encompassed central and dorsal portions of the BNST and extended into surrounding regions including the medial caudate, globus pallidus, posterior and dorsal aspects of the nucleus accumbens, hypothalamus, and anterior and ventral thalamus (Fig. 3*A*). The midbrain cluster was centered on the cerebral aqueduct and enveloped the PAG (Fig. 3*B*) and extended anteriorly into the ventral tegmental area (VTA) and substantia nigra, pars compacta (SNc). Time course data extracted from regions identified using the sustained regressor demonstrated a pattern of deactivation leading up to the picture presentation, with less deactivation for aversive relative to neutral anticipation (Fig. 2).

Table 1.
Anticipatory activity for the comparison of aversive to neutral trials in the 1-regressor model

Region	Brodmann area	Size (mm^3)	Center of mass (*x*, *y*, *z*)	Max *t*	Max *P*
R middle/inferior occipital gyri	18/19	16 472	(32, −89, 3)	8.27	$2.4E^{-10}$
L middle/inferior occipital gyri	18/19	14 576	(−31, −88, −5)	8.58	$8.8E^{-11}$
L posterior cingulate gyrus	23/31	6520	(−3, −34, 35)	4.98	$1.1E^{-5}$
L precuneus	7	5072	(−20, −69, 36)	5.14	$6.7E^{-6}$
L cuneus*	17	3848	(−4, −84, 0)	−5.86	$6.3E^{-7}$
L anterior insula/IFG/OFC	11/47	3464	(−29, 35, −7)	5.16	$6.3E^{-6}$
Rostral cingulate (pACC/aMCC)	24/32	2504	(0, 31, 21)	4.06	$2.1E^{-4}$
Midbrain/PAG	N/A	1904	(−2, −32, −5)	5.21	$5.4E^{-6}$
R fusiform gyrus	37	1864	(28, −52, −10)	3.85	$4.0E^{-4}$
R superior frontal gyrus	6	1048	(2, 4, 53)	3.84	$4.1E^{-4}$
L posterior cingulate gyrus	29	824	(−15, −41, 8)	4.50	$5.3E^{-5}$
L anterior temporal gyrus	38	744	(−39, 26, −23)	4.65	$3.3E^{-5}$
L angular gyrus	39	736	(−39, −74, 25)	4.10	$1.9E^{-4}$
R anterior insula	N/A	456	(34, 26, 0)	3.79	$4.7E^{-4}$
Posterior subgenual cingulate	25	336	(2, 16, −3)	3.81	$4.5E^{-4}$

*All regions showed greater activity for aversive anticipation except the cuneus, which was more active for neutral anticipation. Activation coordinates are provided in MNI space. Maximum *t*- and *P*-values are presented for illustrative purposes and are not intended as providing an independent test of significance. IFG, inferior frontal cortex; OFC, orbitofrontal cortex; pACC, pregenual anterior cingulate cortex; aMCC, anterior mid-cingulate cortex; PAG, periaqueductal gray.

Table 2.
Phasic and sustained anticipatory activity for the comparison of aversive to neutral trials in the 2-regressor model

Region	Brodmann area	Size (mm^3)	Center of mass (*x*, *y*, *z*)	Max *t*	Max *P*
Phasic anticipatory activation					
L middle/inferior occipital gyri	18/19	16 952	(−31, −82, 5)	8.09	$4.2E^{-10}$
R middle/inferior occipital gyri	18/19	15 944	(32, −86, 6)	7.79	$1.1E^{-9}$
L posterior cingulate gyrus	23/31	5840	(−10, −39, 31)	3.57	$9.1E^{-4}$
L cuneus*	17	4824	(−3, −83, −1)	−5.88	$5.9E^{-7}$
R fusiform/parahippocampal gyrus	19/37	2512	(28, −52, −10)	4.34	$8.8E^{-5}$
L orbitofrontal cortex	11	896	(−29, 45, −12)	5.46	$2.4E^{-6}$
L anterior temporal gyrus	38	736	(−38, 25, −24)	4.32	$9.3E^{-5}$
L middle frontal gyrus	6	624	(−39, 0, 45)	3.95	$2.9E^{-4}$
L middle frontal gyrus	6	368	(−24, −9, 52)	3.80	$4.6E^{-4}$
L fusiform/parahippocampal gyrus	19/37	304	(−36, −44, −12)	3.55	$9.6E^{-4}$
L IFG/anterior insula	47	280	(−33, 29, 7)	3.68	$6.6E^{-4}$
Sustained anticipatory activation					
R basal forebrain/BNST	N/A	3016	(6, −4, 1)	4.78	$2.2E^{-5}$
Midbrain/PAG	N/A	1856	(−3, −28, −4)	4.36	$8.2E^{-5}$
L anterior insula	N/A	1768	(−40, 20, 0)	4.08	$2.0E^{-5}$
R anterior insula	N/A	1752	(34, 23, 1)	4.58	$4.1E^{-5}$
R supramarginal gyrus	40	728	(53, −52, 32)	3.97	$2.8E^{-4}$
L angular gyrus*	39	328	(−53, −68, 33)	−4.25	$1.2E^{-4}$

*All regions showed greater activity for aversive anticipation except for the cuneus and angular gyrus, which were more active for neutral anticipation. Activation coordinates are provided in MNI space. Maximum *t*- and *P*-values are presented for illustrative purposes and are not intended as providing an independent test of significance. IFG, inferior frontal gyrus; BNST, bed nucleus of the stria terminalis; PAG, periaqueductal gray.

For active regions previously implicated in the anticipation of aversion (OFC, IFG, anterior insula, basal forebrain/BNST, midbrain/PAG), aversive–neutral parameter estimates for the relevant regressor were extracted from functional clusters and correlated with self-reports of negative affect (PANAS; Watson et al. 1988) and worry (PSWQ; Meyer et al. 1990), constructs of high relevance for clinical anxiety disorders. After applying FDR correction, we found a significant positive correlation between phasic left IFG/anterior insula activity and worry on the PSWQ ($r(41) = 0.43$, $q = 0.009$, $P = 0.033$; all other $r < 0.36$, $q > 0.019$, $P > 0.07$).

Two-Regressor Model: ROI Results

For the anatomically defined rostral cingulate cortex, a Valence (Aversive, Neutral) × Region (pACC, aMCC) × Period (Phasic, Sustained) repeated measures ANOVA revealed main effects of Valence ($F_{1,42} = 9.99$, $P = 0.0029$), Region ($F_{1,42} = 9.67$, $P = 0.0034$), and Period ($F_{1,42} = 13.24$, $P < 0.001$). These main effects were driven by greater activity for aversive versus neutral anticipation, the pACC versus the aMCC, and phasic versus sustained activity, respectively. There were no significant 2-way interactions ($F < 0.02$, $P > 0.90$), but critically, there was a significant Valence × Region × Period interaction ($F_{1,42} = 4.86$, $P = 0.033$). Follow-up tests showed that this interaction resulted from significant phasic pACC activity for the aversive–neutral contrast ($t(42) = 2.71$, $P = 0.010$), and significant sustained activity in the aMCC for aversive relative to neutral anticipation ($t(42) = 2.21$, $P = 0.033$; Fig. 4*A*). Consistent with this ROI analysis, at a threshold of $P < 0.005$ (uncorrected), phasic pACC activity (coordinates = [−2, 38, 14]; $k = 23$) and sustained aMCC activity (coordinates = [3, 7, 33]; $k = 29$) were both observed (Supplementary Fig. S1). For the anatomical ROIs, there were no significant correlations between sustained aMCC activity or phasic pACC activity and scores of either worry on the PSWQ or negative affect on the PANAS ($r < 0.17$; $q > 0.29$, FDR-corrected $P > 0.45$).

An exploratory Valence × Hemisphere × Period repeated measures ANOVA on the anatomically defined amygdala revealed a significant effect of Period ($F_{1,42} = 31.96$), driven by greater amygdala activity for the phasic versus sustained regressor. The Period × Valence interaction trended toward significance ($F_{1,42} = 3.04$, $P = 0.088$), driven by marginally greater aversive–neutral activity for the phasic relative to the sustained regressor, consistent with study hypotheses (Fig. 4*B*; all

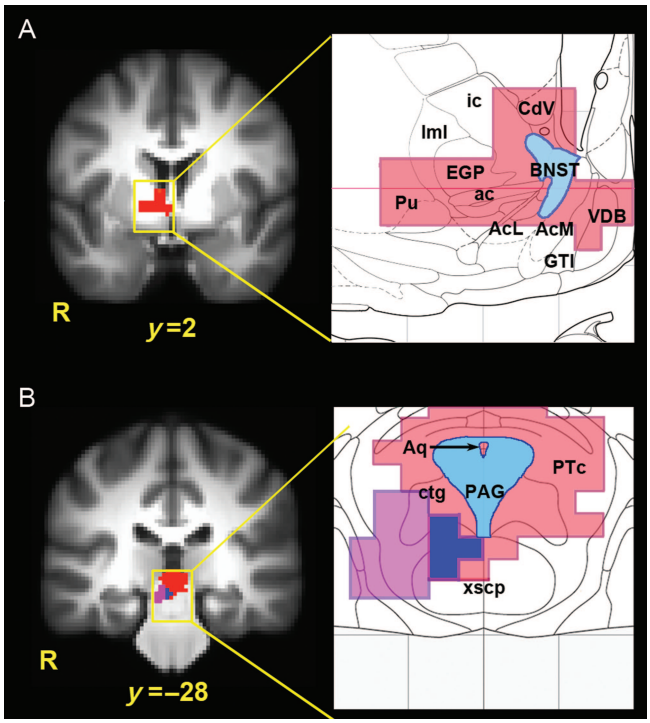

Figure 3. (*A*) Activation of the right basal forebrain during sustained anticipation of aversion, as overlaid on an anatomical atlas (Mai et al. 1998). At $P < 0.05$ (corrected using Monte Carlo simulation), this activation included the dorsal and central BNST (shown in blue), as well as the external globus pallidus (EGP), ventral caudate (CdV), putamen (Pu), vertical limb of the diagonal band (VDB), great terminal island (GTI), and dorsal/posterior portions of the nucleus accumbens (AcL = lateral accumbens core; AcM = medial accumbens shell). ac, anterior commissure; ic, internal capsule, lml, external medullary lamina of the globus pallidus. (*B*) Sustained anticipation of aversion was accompanied by increased midbrain activity (red) overlapping with the anatomical location of the PAG (blue) and pretectal area (PTc) when overlaid on an anatomical atlas (Mai et al. 1998). PPI analysis revealed an overlapping midbrain cluster (purple) showing increased functional coupling with the anterior mid-cingulate cortex during sustained anticipation. All activations shown at $P < 0.05$ (corrected using Monte Carlo simulation). Aq, cerebral aqueduct; ctg, central tegmental tract; xscp, decussation of the cerebellar peduncle. Adapted from Mai et al. 1998.

other $F < 1.95$; $P > 0.17$). Individual differences in the magnitude of aversive–neutral phasic amygdala activation were correlated with negative affect on the PANAS (left: $r(40) = 0.62$, $q < 0.001$, $P < 0.001$; right: $r(41) = 0.42$, $q = 0.0047$, $P = 0.033$) (Fig. 4*C*) and worry on the PSWQ (left: $r(41) = 0.40$, $q = 0.0086$, $P = 0.045$; trend for right: $r(41) = 0.35$, $q = 0.020$, $P = 0.067$; for sustained amygdala responses, $r < |0.27|$, uncorrected $P > 0.07$). The left amygdala correlation with negative affect remained significant when removing shared variance with PSWQ scores ($r_p(40) = 0.60$, uncorrected $P < 0.001$; trend for right amygdala: $r_p(41) = 0.30$, uncorrected $P = 0.053$; all other $r_p < 0.15$, uncorrected $P > 0.35$).

Functional Connectivity Results

The PPI analysis identified the midbrain/PAG as the sole region showing increased positive coupling with the aMCC during aversive versus neutral anticipation (Fig. 3*B*; Supplementary Fig. S2A). This midbrain cluster (center-of-mass = [5, −28, −10]) overlapped with the midbrain cluster seen for sustained anticipation. An analogous PPI analysis using the pACC as a seed region did not identify increased positive coupling with the midbrain (or any other regions) during sustained anticipation of aversion (Supplementary Fig. S2B).

One- versus Two-Regressor Model: Direct Comparison

Phasic aversive–neutral anticipatory activity was significantly weaker for the 2-regressor model than the 1-regressor model in the bilateral anterior insula, aMCC, right basal forebrain, and midbrain, all of which showed sustained anticipatory activity (Supplementary Fig. S3). Additionally, a nearly identical set of regions showed significantly reduced activity for the contrast of aversive–neutral pictures in the 2-regressor model relative to the 1-regressor model (Supplementary Fig. S4). These results show that explicitly modeling sustained anticipatory activity results in reassignment of variance otherwise attributed to phasic anticipatory and picture regressors (Fig. 1, bottom). In addition, voxelwise paired *t*-tests showed that the 2-regressor model accounted for significantly more total variance (R^2) than the 1-regressor model across the brain (Supplementary Fig. S5).

Within-region, pairwise correlations were assessed for a number of regions identified as being active in the 1-regressor model, as well as for the anatomically defined amygdala and rostral cingulate (Supplementary Table S5). Correlations between activity in the 1-regressor model and phasic activity in the 2-regressor model were extremely high ($r = 0.83$–0.94). Correlations between 1-regressor activity and sustained activity were substantially lower, but still positive and significant ($r = 0.33$–0.56), except for the amygdala ($r = 0.06$–0.22). There were, however, no significant within-region correlations between phasic and sustained activity ($r = -0.29$–0.18).

Discussion

We present here results demonstrating dissociable neural circuitry associated with distinct stages in the anticipation of aversion. At the onset of anticipation, the OFC and pACC (and the amygdala for subjects with elevated anxiety symptoms) showed phasic activity in response to aversive cues. A separate set of regions consisting of the anterior insula, aMCC, basal forebrain/BNST, and midbrain/PAG demonstrated greater sustained activity for the anticipation of threat relative to safety. Notably, basal forebrain activity was not observed using a 1-regressor model, but emerged only in the model that included a sustained anticipatory regressor. The aMCC and midbrain/PAG showed increased functional coupling during sustained aversive anticipation, suggesting that this preparatory defensive circuit plays a key role in anticipatory processing. These results underscore the importance of model definition in identifying brain regions involved in unique aspects of aversive anticipation, and encourage further research that acknowledges the importance of distinct constituent processes or temporal stages of anticipation.

One such process important for early anticipatory processing involves rapid threat detection, which we hypothesized would be reflected in phasic amygdala activity, due to this region's critical involvement in vigilance and threat detection (Whalen 1998; LeDoux 2000; Davis and Whalen 2001). Contrary to this hypothesis, such an effect was not observed across all subjects. However, robust correlations with self-report measures of trait negative affect and worry indicated heightened phasic amygdala responses in subjects with

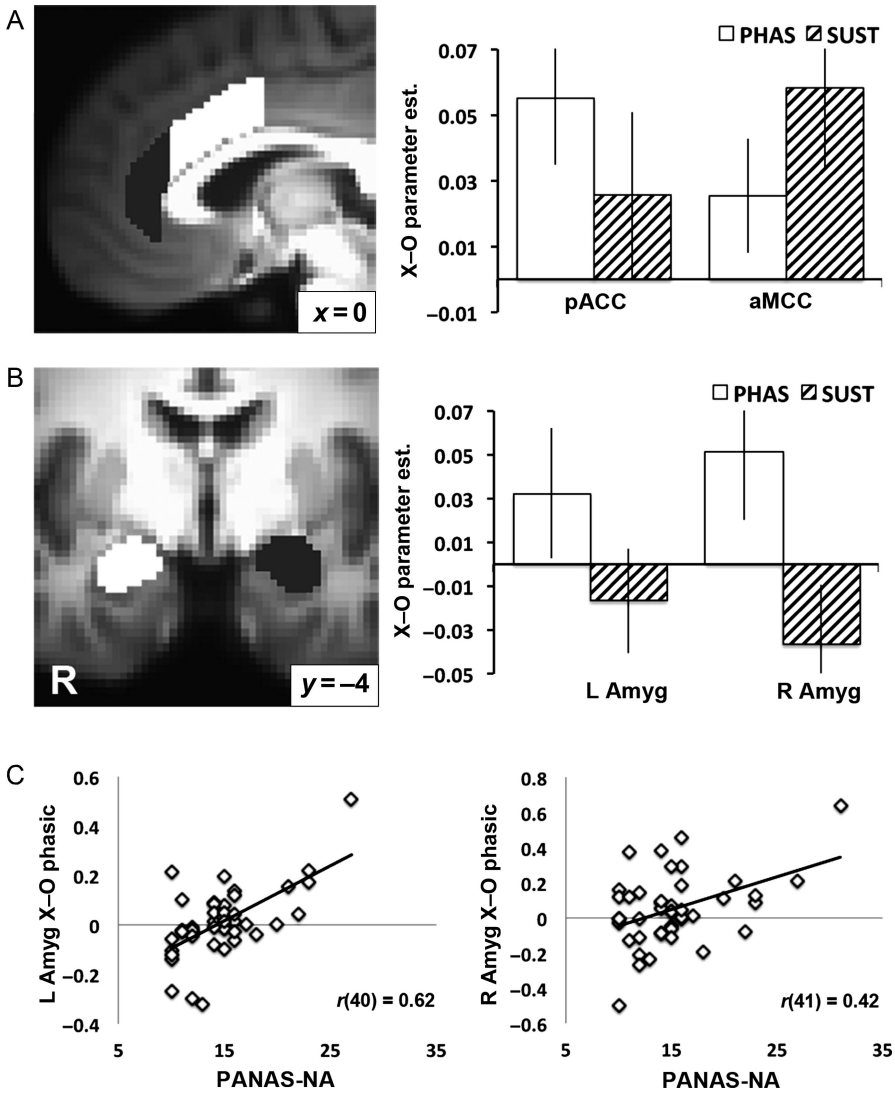

Figure 4. ROI analyses for the anatomically defined rostral cingulate cortex and amygdala. (*A*) The pregenual anterior cingulate cortex (pACC) showed phasic (PHAS) anticipatory activation, while the anterior mid-cingulate cortex (aMCC) showed sustained (SUST) anticipatory activation. (*B*) The amygdala (AMYG) showed marginally greater phasic relative to sustained anticipatory activation. For (*A*) and (*B*), error bars show standard error of the mean. (*C*) Scatter plots reflecting significant correlations between phasic amygdala activation and negative affect (NA) scores on the Positive and Negative Affect Schedule (PANAS). One regression outlier (i.e., studentized residual with Bonferonni corrected $P < 0.05$) was removed from the left amygdala correlation, which thus includes only 42 data points.

elevated anxiety symptoms. Amygdala activity has been observed in aversive anticipation paradigms (Phelps et al. 2001; Mackiewicz et al. 2006; Nitschke et al. 2006) but not consistently (Mechias et al. 2010). The use here of an anticipatory model with multiple regressors revealed a role for the amygdala in early stages of anticipation for subjects with heightened anxiety symptoms that may be overlooked in studies that fail to adequately parse the anticipatory epoch. Stronger phasic amygdala effects might be seen across all individuals with the use of a more aversive stimulus that induces greater anticipatory anxiety (e.g., shock), but it is of theoretical interest that the less potent stimuli used here so robustly engaged the amygdala in subjects with elevated anxiety symptoms (Lissek et al. 2006).

Sustained aversive anticipation was associated with increased activity in a basal forebrain region encompassing the BNST. Animal research has revealed a role for the BNST in increased anxious responding and vigilance under conditions of sustained, unpredictable threat (Davis et al. 2010). Recent neuroimaging studies suggest a comparable role for the BNST in humans, with activity observed for increasing spatial or temporal proximity to threat (Mobbs et al. 2010; Somerville et al. 2010) and for an unpredictable threatening context (Straube et al. 2007; Alvarez et al. 2011; Somerville et al. 2012). Notably, although this basal forebrain cluster enveloped much of the dorsal/central BNST, it included multiple surrounding regions, as depicted in Figure 3. Consistent with recent findings (Somerville et al. 2010, 2012; Alvarez et al. 2011), sustained anticipation of aversion also activated the anterior insula, which sends direct projections to the BNST and other extended amygdala subregions (McDonald et al. 1999). Together, these regions may be part of a core circuit involved in long-duration threat responses in anticipation of aversive events.

Research in animal models has highlighted a central role for the PAG in the expression of both active (fight/flight) and

passive (freezing) defensive behavior (reviewed in Bandler et al. 2000). Human neuroimaging studies have long emphasized the importance of the PAG in the experience and modulation of pain, but more recent work has implicated this region in a wider variety of tasks including the anticipation of pain, as well as responses to other emotional stimuli (Ploner et al. 2010; Linnman et al. 2012). The current observation of sustained midbrain activity centered on the PAG extends the scope of previous studies to include a role in anticipation of negative outcomes other than pain, and is conceptually consistent with recent studies reporting midbrain/PAG activation during conditions of proximal (relative to distal) threat (Mobbs et al. 2007, 2009, 2010). The anterior portion of this midbrain cluster overlaps with the location of the VTA and SNc, the primary sources of dopaminergic neurons that project to the striatum and PFC (Bromberg-Martin et al. 2010). Although these dopaminergic nuclei are typically highlighted in studies of reward anticipation and delivery, recent evidence demonstrates a comparable role for aversive events, suggesting the VTA and SNc may code for motivational salience in addition to motivational value (Bromberg-Martin et al. 2010).

It is important to take note of several factors that preclude unequivocal statements regarding the involvement of the BNST and PAG during this task: Their small sizes, the presence of other small subcortical nuclei surrounding these structures, and in the case of the BNST, partial volume effects compounded by the nearby cerebral ventricles (Alvarez et al. 2011). We attempted to address these challenges by utilizing a more precise nonlinear registration technique (see Materials and Methods) and by noting the consistency of the current results with the growing literature on BNST and PAG activation in human subjects (Mobbs et al. 2007, 2009, 2010; Straube et al. 2007; Somerville et al. 2010, 2012; Alvarez et al. 2011). That being said, future work using high-resolution imaging (Alvarez et al. 2011), tractography-based segmentation (Saygin et al. 2011), or pharmacological manipulations will be critical in determining the precise subcortical structures involved in aversive anticipation.

Robust anticipatory activity spanning the pACC and aMCC was observed for the 1-regressor model, whereas anatomical ROI analysis for the 2-regressor model revealed phasic anticipatory activity in the pACC and sustained activity in the aMCC (see also Supplementary Fig. S1). Although activation along the extent of the rostral cingulate has been reported in studies of aversive anticipation, the aMCC (often denoted as dorsal ACC) is the most consistently activated region in such studies (Mechias et al. 2010). This sustained activity is consistent with previous studies that have shown elevated aMCC activity with increasing threat proximity (Mobbs et al. 2010) and elevated anxiety ratings during a sustained anticipatory period (Straube et al. 2009). Based on common recruitment of the aMCC across a variety of tasks requiring intentional control under conditions of some uncertainty, as well as its unique structural connectivity profile, Shackman et al. (2011) proposed that the aMCC enacts "adaptive control" by integrating incoming information about negative reinforcers and, through its efferent connections, modulating subsequent behavior to avoid negative outcomes. Our observation of increased functional connectivity between the aMCC and midbrain during aversive anticipation provides support for the adaptive control hypothesis, and is consistent with known anatomical connections (An et al. 1998) and a previous report of enhanced aMCC–PAG functional connectivity in peri-threat encounters (Mobbs et al. 2009).

Quantitative comparisons of the 1- and 2-regressor models suggested 2 distinct sources for the activity identified using the sustained regressor. Relative to the 1-regressor model, we observed reduced activity in the 2-regressor model for the phasic anticipation and picture conditions in a set of regions almost completely overlapping with those regions demonstrating sustained anticipatory activity (Supplementary Figs S3 and S4). This suggests that the sustained activity reported here largely reflects reassignment of variance that was previously (and perhaps inappropriately) attributed to 1 of these other 2 conditions. In addition to this shifting variance, activity that was assigned to the error term (or baseline) for the 1-regressor model was modeled as sustained activity for the 2-regressor model, as reflected in widespread increases in overall variance accounted for by the 2-regressor model. These results, as well as the identification of a large basal forebrain cluster only in the 2-regressor model, highlight the benefits of parsing anticipatory brain activity into temporal stages that may be associated with distinct psychological processes.

Investigation of time course activity revealed, somewhat unexpectedly, that sustained condition differences actually resulted from less deactivation for aversive relative to neutral anticipation. While we can only speculate about the associated psychological processes, this pattern of deactivation is consistent with active dampening or regulation of activity in these regions, with greater dampening for the safe, neutral condition. In several of these regions, activity appeared to still be decreasing at the end of the longest anticipatory epochs (8 s after cue offset). This observation suggests that longer anticipatory periods may allow for even more robust differences between conditions, particularly in regions known to be critical for long-duration anxious responding (e.g., the BNST; Davis et al. 2010; Somerville et al. 2012).

The identification of brain regions with dissociable activity during different temporal stages of aversive anticipation is of high relevance for the neurobiological investigation of clinical anxiety. A common theme across theoretical perspectives on anxiety disorders is that excessive, aberrant anticipation of negative events is at the core of anxious pathology (Barlow 2000; Borkovec 2002; Nitschke et al. 2009). The regions identified in the current study have previously been implicated in neuroimaging studies of aversive anticipation in clinical anxiety (Lorberbaum et al. 2004; Straube et al. 2007; Nitschke et al. 2009; Simmons et al. 2011) and trait anxiety (Simmons et al. 2006; Stein et al. 2007; Somerville et al. 2010; Carlson et al. 2011), as well as animal models of anxiety (Kalin et al. 2004; Davis et al. 2010; Fox et al. 2010). The current study provides a useful framework for investigating the anticipation of negative outcomes in anxiety disorders, making it possible to probe brain function during distinct stages of anticipation that may be differentially implicated in a particular disorder. For example, individuals or disorders marked by hypervigilance may demonstrate exaggerated phasic anticipatory activation of the amygdala, while others associated with reduced fear inhibition during objectively safe conditions may show reduced deactivation during neutral anticipation in regions typically associated with sustained condition differences (Nitschke et al. 2009).

As noted above, regions found here for phasic and sustained threat anticipation show striking overlap with regions involved in responding to distal and proximal threat, respectively (Mobbs et al. 2007, 2009, 2010). For example, Mobbs et al. (2010) reported activation of the OFC and PCC for tarantulas that were more distant, while the PAG, BNST, anterior insula, and aMCC showed increased activity when participants were in close physical proximity to tarantulas. Also of high relevance for the current work, instructed contextual fear conditioning in virtual reality environments resulted in transient amygdala activity following threat cues, while exposure to unpredictably threatening contexts resulted in sustained activation of the BNST and anterior insula (Alvarez et al. 2011). This convergence of results across studies suggests that each of these paradigms engages similar functional mechanisms, despite several discrepancies including the nature of the task and threat stimulus, explicit instructions to participants, and time course of threat exposure. Future work is needed to delineate the core mechanisms common to the monitoring of proximal threat, exposure to a threatening environmental context, and the anticipation of negative events, as well as to clarify the distinct psychological and neural processes unique to each task.

In summary, we provide evidence for dissociable brain regions showing phasic activity to anticipatory cues versus sustained anticipatory responses. Although it is clear that modeling sustained activity is important for long-duration anticipatory periods or different contexts (e.g., Straube et al. 2007; Alvarez et al. 2011; Somerville et al. 2012), we show here that there are striking benefits to explicitly modeling both phasic and sustained anticipatory responses even for a relatively short anticipatory period. The identification of neural processes involved in distinct temporal stages of anticipation may pave the way for future, targeted investigations of specific psychological processes (e.g., threat detection, attentional processes, hyperarousal, subjective emotional awareness, emotion regulation) that contribute to adaptive anticipatory function across these stages. Furthermore, extensions of this work to clinical anxiety may allow researchers to shed light on specific anticipatory processes that are altered in these disorders.

Supplementary Material

Supplementary material can be found at: http://www.cercor.oxfordjournals.org/

Funding

This work was supported by the National Institutes of Health (R01-MH74847, K02-MH082130, and K08-MH63984 to J.B.N.; T32-MH018931 for D.W.G.) and by a National Science Foundation Graduate Research Fellowship to D.W.G.

Notes

We thank Dan McFarlin, Tammi Kral, Dave Perlman, Daniel Bradford, Michael Anderle, and Ron Fisher for helpful suggestions and technical assistance. *Conflict of Interest*: None declared.

References

Alvarez RP, Chen G, Bodurka J, Kaplan R, Grillon C. 2011. Phasic and sustained fear in humans elicits distinct patterns of brain activity. Neuroimage. 55:389–400.

An X, Bandler R, Ongur D, Price JL. 1998. Prefrontal cortical projections to longitudinal columns in the midbrain periaqueductal gray in macaque monkeys. J Comp Neurol. 401:455–479.

Bandler R, Keay KA, Floyd N, Price J. 2000. Central circuits mediating patterned autonomic activity during active vs. passive emotional coping. Brain Res Bull. 53:95–104.

Barlow DH. 2000. Unraveling the mysteries of anxiety and its disorders from the perspective of emotion theory. Am Psychol. 55:1247–1263.

Birbaumer N, Elbert T, Canavan AGM, Rockstroh B. 1990. Slow potentials of the cerebral cortex and behavior. Physiol Rev. 70:1–41.

Böcker KBE, Baas JMP, Kenemans KL, Verbaten MN. 2001. Stimulus-preceding negativity induced by fear: a manifestation of affective anticipation. Int J Psychophysiol. 43:77–90.

Borkovec TD. 2002. Life in the future versus life in the present. Clin Psychol Sci Prac. 9:76.–80.

Bromberg-Martin ES, Matsumoto M, Hikosaka O. 2010. Dopamine in motivational control: rewarding, aversive, and alerting. Neuron. 68:815–834.

Carlson JM, Greenberg T, Rubin D, Mujica-Parodi LR. 2011. Feeling anxious: anticipatory amygdalo-insular response predicts the feeling of anxious anticipation. Soc Cogn Affect Neurosci. 6:74–81.

Cox RW. 1996. AFNI: software for analysis and visualization of functional magnetic resonance neuroimages. J Biomed Inform. 29:162–173.

Craig AD. 2002. How do you feel? Interoception: the sense of the physiological condition of the body. Nat Rev Neurosci. 3:655–666.

Craig AD. 2009. How do you feel–now? The anterior insula and human awareness. Nat Rev Neurosci. 10:59–70.

Critchley HD. 2005. Neural mechanisms of autonomic, affective, and cognitive integration. J Comp Neurol. 493:154–166.

Critchley HD. 2009. Psychophysiology of neural, cognitive and affective integration: fMRI and autonomic indicants. Int J Psychophysiol. 73:88–94.

Critchley HD, Wiens S, Rotshtein P, Ohman A, Dolan RJ. 2004. Neural systems supporting interoceptive awareness. Nat Neurosci. 7:189–195.

Davis M, Walker DL, Miles L, Grillon C. 2010. Phasic vs. sustained fear in rats and humans: role of the extended amygdala in fear vs. anxiety. Neuropsychopharmacology. 35:105–135.

Davis M, Whalen PJ. 2001. The amygdala: vigilance and emotion. Mol Psychiatry. 6:13–34.

Drabant EM, Kuo JR, Ramel W, Blechert J, Edge MD, Cooper JR, Goldin PR, Hariri AR, Gross JJ. 2011. Experiential, autonomic, and neural responses during threat anticipation vary as a function of threat intensity and neuroticism. Neuroimage. 55:401–410.

First MB, Spitzer RL, Gibbon M, Williams JBW. 2002. Structured Clinical Interview for DSM-IV-TR Axis I Disorders, Research Version (SCID-I). New York: Biometrics Research.

Fox AS, Shelton SE, Oakes TR, Converse AK, Davidson RJ, Kalin NH. 2010. Orbitofrontal cortex lesions alter anxiety-related activity in the primate bed nucleus of stria terminalis. J Neurosci. 30:7023–7027.

Friston KJ, Büchel C, Fink GR, Morris J, Rolls E, Dolan RJ. 1997. Psychophysiological and modulatory interactions in neuroimaging. Neuroimage. 6:218–229.

Herwig U, Baumgartner T, Kaffenberger T, Bruhl A, Kottlow M, Schreiter-Gasser U, Abler B, Jancke L, Rufer M. 2007. Modulation of anticipatory emotion and perception processing by cognitive control. Neuroimage. 37:652–662.

Kalin NH, Shelton SE, Davidson RJ. 2004. The role of the central nucleus of the amygdala in mediating fear and anxiety in the primate. J Neurosci. 24:5506–5515.

Kalisch R, Wiech K, Critchley HD, Dolan RJ. 2006. Levels of appraisal: a medial prefrontal role in high-level appraisal of emotional material. Neuroimage. 30:1458–1466.

Kalisch R, Wiech K, Critchley HD, Seymour B, O'Doherty JP, Oakley DA, Allen P, Dolan RJ. 2005. Anxiety reduction through detachment: subjective, physiological, and neural effects. J Cogn Neurosci. 17:874–883.
Kumari V, ffytche DH, Das M, Wilson GD, Goswami S, Sharma T. 2007. Neuroticism and brain responses to anticipatory fear. Behav Neurosci. 121:643–652.
Lang PJ, Bradley MM, Cuthbert BN. 2008. International affective picture system (IAPS): affective ratings of pictures and instruction manual. Technical Report A-8. Gainesville (FL): University of Florida.
LeDoux JE. 2000. Emotion circuits in the brain. Annu Rev Neurosci. 23:155–184.
Linnman C, Moulton EA, Barmettler G, Becerra L, Borsook D. 2012. Neuroimaging of the periaqueductal gray: state of the field. Neuroimage. 60:505–522.
Lissek S, Pine DS, Grillon C. 2006. The strong situation: a potential impediment to studying the psychobiology and pharmacology of anxiety disorders. Biol Psychol. 72:265–270.
Lorberbaum JP, Kose S, Johnson MR, Arana GW, Sullivan LK, Hamner MB, Ballenger JC, Lydiard RB, Brodrick PS, Bohning DE *et al*. 2004. Neural correlates of speech anticipatory anxiety in generalized social phobia. Neuroreport. 15:2701–2705.
Mackiewicz KL, Sarinopoulos I, Cleven KL, Nitschke JB. 2006. The effect of anticipation and the specificity of sex differences for amygdala and hippocampus function in emotional memory. Proc Natl Acad Sci USA. 103:14200–14205.
Mai JK, Assheuer J, Paxinos G. 1998. Atlas of the human brain. San Diego, CA: Academic Press. Electronic version 1.0
McDonald AJ, Shammah-Lagnado SJ, Shi C, Davis M. 1999. Cortical afferents to the extended amygdala. Ann N Y Acad Sci. 877: 309–338.
Mechias ML, Etkin A, Kalisch R. 2010. A meta-analysis of instructed fear studies: implications for conscious appraisal of threat. Neuroimage. 49:1760–1768.
Meyer TJ, Miller ML, Metzger RL, Borkovec TD. 1990. Development and validation of the Penn State Worry Questionnaire. Behav Res Ther. 28:487–495.
Milad MR, Quirk GJ, Pitman RK, Orr SP, Fischl B, Rauch SL. 2007. A role for the human dorsal anterior cingulate cortex in fear expression. Biol Psychiatry. 62:1191–1194.
Mobbs D, Marchant JL, Hassabis D, Seymour B, Tan G, Gray M, Petrovic P, Dolan RJ, Frith CD. 2009. From threat to fear: the neural organization of defensive fear systems in humans. J Neurosci. 29:12236–12243.
Mobbs D, Petrovic P, Marchant JL, Hassabis D, Weiskopf N, Seymour B, Dolan RJ, Frith CD. 2007. When fear is near: threat imminence elicits prefrontal-periaqueductal gray shifts in humans. Science. 317:1079–1083.
Mobbs D, Yu R, Rowe JB, Eich H, FeldmanHall O, Dalgleish T. 2010. Neural activity associated with monitoring the oscillating threat value of a tarantula. Proc Natl Acad Sci USA. 107:20582–20586.
Nitschke JB, Sarinopoulos I, Mackiewicz KL, Schaefer HS, Davidson RJ. 2006. Functional neuroanatomy of aversion and its anticipation. Neuroimage. 29:106–116.
Nitschke JB, Sarinopoulos I, Oathes DJ, Johnstone T, Whalen PJ, Davidson RJ, Kalin NH. 2009. Anticipatory activation in the amygdala and anterior cingulate in generalized anxiety disorder and prediction of treatment response. Am J Psychiatry. 166:302–310.
Phelps EA, O'Connor KJ, Gatenby JC, Gore JC, Grillon C, Davis M. 2001. Activation of the left amygdala to a cognitive representation of fear. Nat Neurosci. 4:437–441.
Ploghaus A, Tracey I, Gati JS, Clare S, Menon RS, Matthews PM, Rawlins JN. 1999. Dissociating pain from its anticipation in the human brain. Science. 284:1979–1981.
Ploner M, Lee MC, Wiech K, Bingel U, Tracey I. 2010. Prestimulus functional connectivity determines pain perception in humans Proc Natl Acad Sci USA. 107:355–360.
Saygin ZM, Osher DE, Augustinack J, Fischl B, Gabrieli JDE. 2011. Connectivity-based segmentation of human amygdala nuclei using probabilistic tractography. Neuroimage. 56:1353–1361.
Shackman AJ, Salomons TV, Slagter HA, Fox AS, Winter JJ, Davidson RJ. 2011. The integration of negative affect, pain and cognitive control in the cingulate cortex. Nat Rev Neurosci. 12:154–167.
Simmons A, Strigo I, Matthews SC, Paulus MP, Stein MB. 2006. Anticipation of aversive visual stimuli is associated with increased insula activation in anxiety-prone subjects. Biol Psychiatry. 60:402–409.
Simmons AN, Stein MB, Strigo IA, Arce E, Hitchcock C, Paulus MP. 2011. Anxiety positive subjects show altered processing in the anterior insula during anticipation of negative stimuli. Hum Brain Mapp. 32:1836–1846.
Somerville LH, Wagner DD, Wig GS, Moran JM, Whalen PJ, Kelley WM. 2012. Interactions between brief and persistent neural signals support the generation and regulation of anxious emotion. Cereb Cortex. Epub ahead of print. doi: 10.1093/cercor/bhr373.
Somerville LH, Whalen PJ, Kelley WM. 2010. Human bed nucleus of the stria terminalis indexes hypervigilant threat monitoring. Biol Psychiatry. 68:416–424.
Stein MB, Simmons AN, Feinstein JS, Paulus MP. 2007. Increased amygdala and insula activation during emotion processing in anxiety-prone subjects. Am J Psychiatry. 164:318–327.
Straube T, Mentzel HJ, Miltner WH. 2007. Waiting for spiders: brain activation during anticipatory anxiety in spider phobics. Neuroimage. 37:1427–1436.
Straube T, Schmidt S, Weiss T, Mentzel H-J, Miltner WHR. 2009. Dynamic activation of the anterior cingulate cortex during anticipatory anxiety. Neuroimage. 44:975–981.
Vogt BA. 2005. Pain and emotion interactions in subregions of the cingulate gyrus. Nat Rev Neurosci. 6:533–544.
Wager TD, Rilling JK, Smith EE, Sokolik A, Casey KL, Davidson RJ, Kosslyn SM, Rose RM, Cohen JD. 2004. Placebo-induced changes in fMRI in the anticipation and experience of pain. Science. 303:1162–1167.
Watson D, Clark LA, Tellegen A. 1988. Development and validation of brief measures of positive and negative affect – the PANAS scales. J Pers Soc Psychol. 54:1063–1070.
Whalen PJ. 1998. Fear, vigilance, and ambiguity: initial neuroimaging studies of the human amygdala. Curr Dir Psychol Sci. 7:177–188.